

## Use of Curcuma and Curcumin as a Green Corrosion Inhibitors for carbon Steel in Sulfuric Acid

E.A. Flores-Frias<sup>1</sup>, V. Barba<sup>2</sup>, M.A. Lucio-Garcia<sup>3</sup>, R. Lopez-Cecenes<sup>1</sup>, J. Porcayo-Calderon<sup>1</sup>, J.G. Gonzalez-Rodriguez<sup>1,\*</sup>

<sup>1</sup> Universidad Autonoma del Estado de Morelos, CIICAp, Av. Universidad 1001-62209-Cuernavaca, Mor., Mexico

<sup>2</sup> Universidad Autonoma del Estado de Morelos, CIQ, Av. Universidad 1001-62209-Cuernavaca, Mor., Mexico

<sup>3</sup> Universidad Autonoma de Yucatan, Facultad de Quimica, C. 43 No. 613 X C. 90, Inalámbrica 97069, Mérida, Yucatán, México.

\*E-mail: [ggonzalez@uaem.mx](mailto:ggonzalez@uaem.mx)

Received: 1 March 2019 / Accepted: 4 April 2019 / Published: 10 May 2019

---

The use of *Curcuma* (*Curcuma longa* L.) extract as a green corrosion inhibitor for 1018 carbon steel in 0.5 M H<sub>2</sub>SO<sub>4</sub> solution has been evaluated by using weight loss tests, potentiodynamic polarization curves and electrochemical impedance spectroscopy measurements. Results have shown that *Curcuma longa* L. decreased the weight loss by one and the corrosion current density values by two orders of magnitudes. Results of free energy suggest physical adsorption on to the steel surface obeying a Langmuir type of adsorption isotherm. Polarization studies give evidence that *Curcuma longa* L. extract behaves as a predominantly cathodic type of inhibitor, and its efficiency increases with increasing its concentration, reaching a maximum value of 90%.

---

**Keywords:** Carbon steel, acid corrosion, green inhibitor.

### 1. INTRODUCTION

Corrosion of metals is a phenomenon that humankind has to deal with every single day since it affects all metals exposed to an aqueous solution. One of the situations where corrosion is present is in the chemical cleaning and pickling where a rapid deterioration of metals in contact with acids such as hydrochloric, sulfuric or nitric due to their aggressiveness. Therefore, different ways to fight metals corrosions is of big concern due to the big economical loses and accidents caused by metals degradation. One of the most popular methods to mitigate corrosion is the use of organic inhibitors containing heteroatoms, such as nitrogen-base materials and their derivatives. Sulphur-containing compounds,

aldehydes, thioaldehydes and acetylenic compounds contain heteroatoms and lone electron pairs, which allow for their adsorption on to the steel surface [1-5]. Here it should be noted that some inhibitors contain nitrogen and sulphur functionalities that can induce some harmful impacts on the public health and environment [2-5]. Moreover, these inhibitors are quite expensive. Considering the existing environmental regulations, it can be stated that the development of cheap, non-toxic and environmental-friendly natural products as green corrosion inhibitors is very important and challenging [6-12] since they contain heteroatoms which can shear their electrons with the empty orbitals of metal ions to form compounds which are adsorbed on the metallic surface.

*Curcuma longa L.* also known as “turmeric” is an herbaceous plant originally from South and Southeast tropical-Asia [13]. It contains commercially interesting compounds based on the production of natural pigment (curcumin), oleoresins, and used as a spice [14]. The dry rhizome of *Curcuma longa L.* contains around 2–5% of essential oil and between 0.02–2% of curcumin. *Curcuma longa L.* has been used for a very long time as spice and agent to give cooler as well as popular medicine for the treatment of several diseases. Turmeric rhizome extracts have medicinal properties that prevent various diseases due to its antioxidant [15] antimicrobial [16] anti-viral properties [17] showing also fungicidal activity [18, 19], anti-Alzheimer [20] anti-mutagenic and anti-carcinogenic qualities [21]. What is more it has been also reported that *Curcuma longa L.* extracts have been used to treat snake bites [22]. Curcumin ( $C_{21}H_{20}O_6$ ), is the main polyphenol found in the *Curcuma longa L.* and it is the main responsible for its medicine and pharmaceutical properties, and it is present together with demethoxycurcumin and bisdemethoxycurcumin, which have chemical structures as given in Fig. 1. Thus, the goal of this research is to evaluate the use of *Curcuma longa L.* extract and Curcumin as green corrosion inhibitors for carbon steel in sulfuric acid.

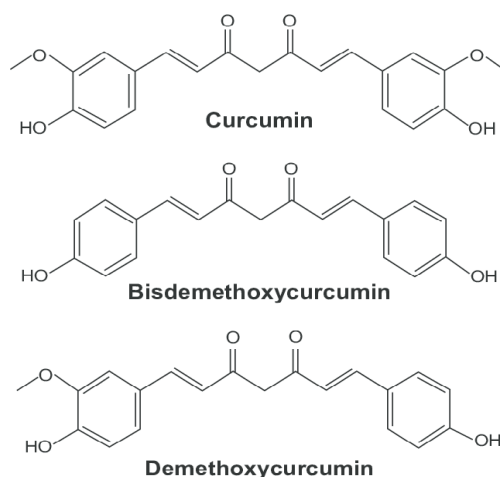


**Figure 1.** Chemical structure of main compounds contained in *Curcuma longa L.*

## 2. EXPERIMENTAL PROCEDURE

### 2.1 Testing material

Material used in this research work includes 1018 carbon steel bars having 6.00 mm in diameter and 10.00 mm long containing containing 0.14% C, 0.90% Mn, 0.30% S, 0.030% P and as balance Fe. For

the electrochemical tests, specimens were encapsulated in a polymeric resin, abraded with 600 grade emerging paper, washed, and degreased with acetone.

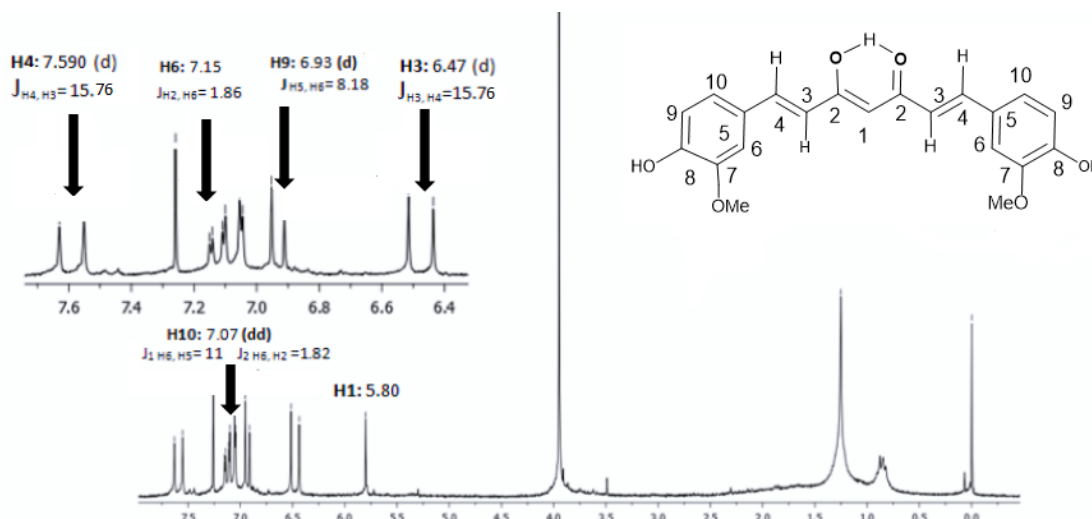


**Figure 2.**  $^1\text{H}$ -NMR spectrum in  $\text{CDCl}_3$  for curcumin.

## 2.2 Testing solution

Solution used for this work includes 0.5 M  $\text{H}_2\text{SO}_4$  prepared with analytical grade reagents at room temperature, around  $25^\circ\text{C}$ . *Curcuma longa L.* extract was added in different concentrations to this solution. To obtain the extract, fresh *Curcuma longa L.* bulbs were obtained in a local market. They were crushed and macerated in methanol during 30 days until methanol was evaporated, obtaining a solid paste. After this, a small amount of methanol was added to this solid and used as a stock solution and used then for preparation of the desired concentrations by dilution. The powder belonging to the turmeric rhizome (920 g) was used for the extraction of Curcumin by maceration, using ethanol as solvent. The solvent was removed by using an evaporator then, the solid was recrystallized in ethanol (80 mL), at the end it was filtered to obtain an orange-red solid which was dried completely, the yield obtained was 6 g. Molecule characterization by  $^1\text{H}$  and  $^{13}\text{C}$  NMR, was performed in a Bruker Avance III de 400 MHz equipment. For the weight loss experiments, specimens were immersed in the electrolyte during 72 hours. Tests were performed by triplicate at room temperature ( $25^\circ\text{C}$ ), by using a hot plate. To calculate the weight loss measurements,  $\Delta W$ , it was used following equation:

$$\Delta W = (m_1 - m_2) / A \quad (1)$$

were  $m_1$  is the mass of the specimen before corrosion,  $m_2$  the mass of the specimen after corrosion, and  $A$  the exposed area of the specimen. For the weight loss tests, inhibitor efficiency,  $IE$ , was calculated as follows:

$$IE (\%) = 100 (\Delta W_1 - \Delta W_2) / \Delta W_1 \quad (2)$$

were  $\Delta W_1$  is the weight loss without inhibitor, and  $\Delta W_2$  the weight loss with inhibitor.

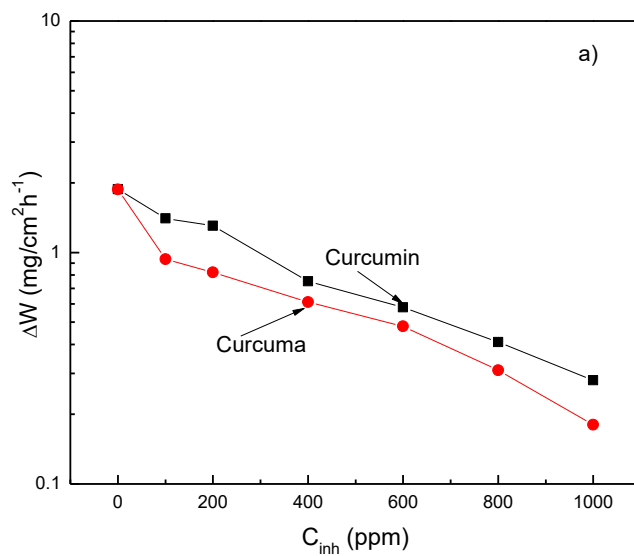


**Figure 3.** Weight loss results as a function of *Curcuma longa L.* and Curcumin for 1018 carbon steel in 0.5 M  $\text{H}_2\text{SO}_4$ .

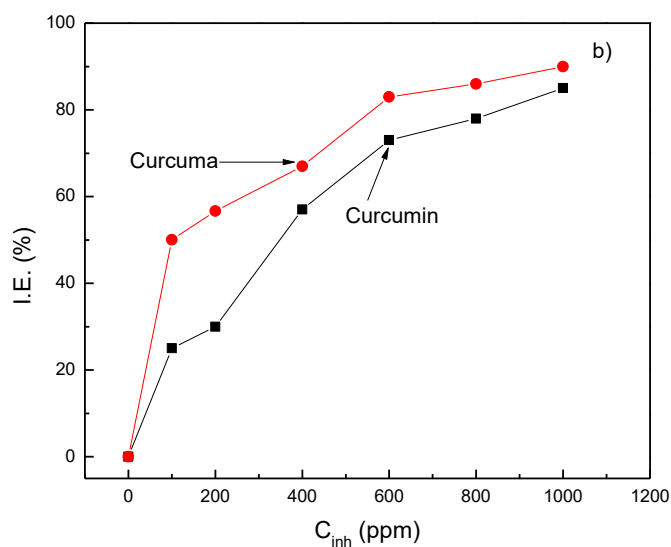


**Figure 4.** Inhibitor efficiency values as a function of *Curcuma longa L.* and Curcumin for 1018 carbon steel in 0.5 M  $\text{H}_2\text{SO}_4$ .

### 2.3 Electrochemical tests.

Electrochemical techniques employed included potentiodynamic polarization curves and electrochemical impedance spectroscopy measurements, EIS. For this, a three electrodes cell was used, with a Saturated calomel electrode (SCE) and a graphite rod as reference and auxiliary electrodes respectively. Before starting the tests, specimens was allowed to reach a stable open circuit potential

value,  $E_{\text{corr}}$ . Polarization curves were started by polarizing the specimen cathodically, 500 mV more cathodic than the  $E_{\text{corr}}$  value, and it ended 500 mV more anodic, recorded at a constant sweep rate of 1 mV/s. Corrosion current density values,  $I_{\text{corr}}$ , were obtained by using Tafel extrapolation. Electrochemical impedance spectroscopy tests were carried out at the open circuit potential value by applying a sinusoidal signal 10 mV peak to peak in a frequency interval of 100 mHz-100 KHz. An ACM potentiostat controlled by a desk top computer was used for the polarization curves, whereas for the EIS measurements, a model PC4 300 Gamry potentiostat was used. After the experiment, surface specimens were analyzed in a LEO VP 1450 high vacuum Scanning electron microscope (SEM) whereas micro chemical analysis was carried out with an X ray energy analyzer (EDX) attached to it.

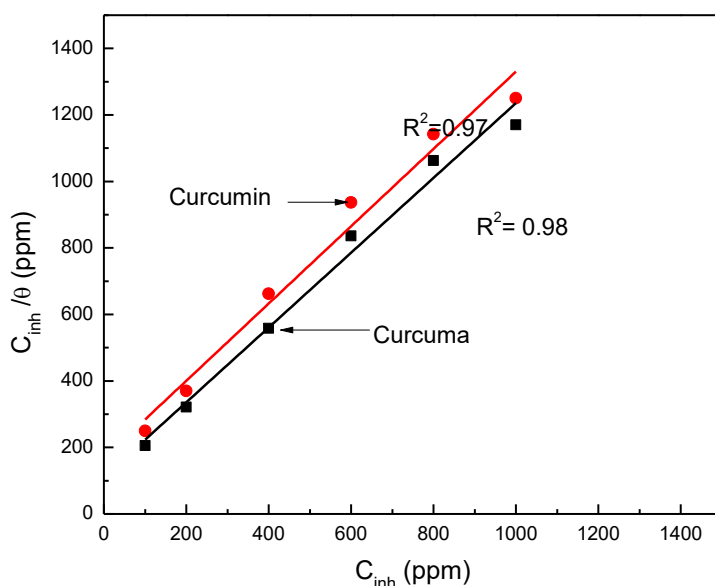


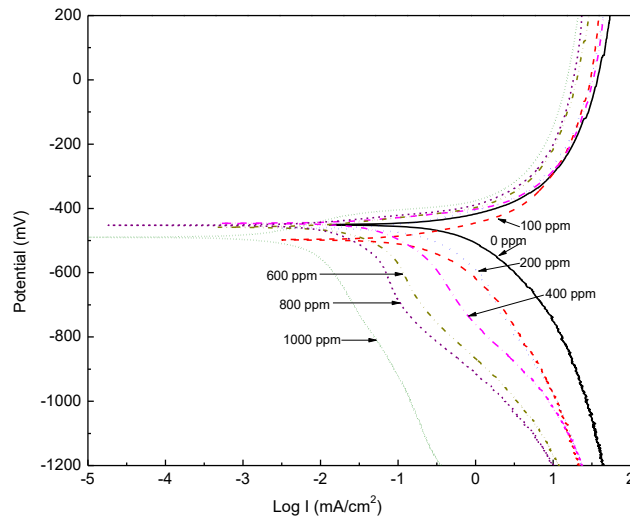
**Figure 5.** Langmuir type of adsorption isotherm for 1018 carbon steel in 0.5 M  $\text{H}_2\text{SO}_4$  corroded in presence of *Curcuma longa L.* and Curcumin.

### 3. RESULTS AND DISCUSSION

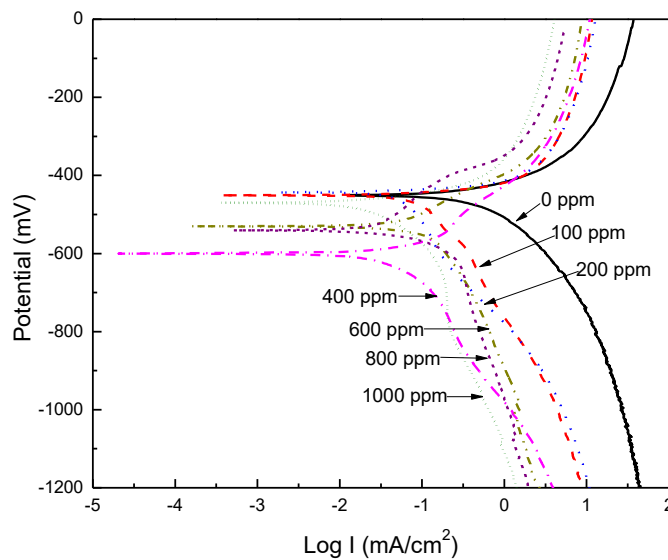
#### 3.1 Curcumine characterization

Fig. 2. shows the  $^1\text{H}$  NMR spectrum for curcumin, in which Hydrogens atoms position is expressed through the chemical shifts of the signals, as well as the corresponding coupling constants. As observed in Fig. 2. the signal for H-1 was shifted of  $\delta$  5.80 ppm as singlet, the H-3 signal is observed in  $\delta$  6.47 ppm as a doublet with a coupling constant of 15.76 Hz. In comparison the signal for H-4 is shifted to  $\delta$  7.590 ppm with the same constant. Finally, the signals for the aromatic hydrogens are shifted from 6.90 to 7.15 ppm.

3.2 Weight loss tests.



**Figure 6.** Effect of *Curcuma longa L.* concentration on the polarization curves for 1018 carbon steel in 0.5 M H<sub>2</sub>SO<sub>4</sub>.



**Figure 7.** Effect of Curcumin concentration on the polarization curves for 1018 carbon steel in 0.5 M H<sub>2</sub>SO<sub>4</sub>.

The change in the weight loss and inhibitor efficiency for 1018 carbon steel with *Curcuma longa L.* and Curcumin concentration is given in Figs. 3 and 4 respectively. It can be seen that in both cases, the weight loss decreases whereas the inhibitor efficiency value increases as the inhibitor concentration

increases, however, the weight losses obtained with *Curcuma longa L.* were lower than those obtained with Curcumin, and, thus, obtaining higher inhibitor efficiency values for the formes, obtaining a maximum efficiency of 90% with the addition of 1000 ppm and 85 for *Curcuma longa L.* and Curcumin respectively. This is due to the existence of compounds with heterocyclic structures which contain heteroatoms such as carbon and oxygen, as shown in Fig.1, which form compounds which are adsorbed on to the steel surface [15-22]. Kairi and Kassim [23] evaluated the effect of *Curcuma longa L.* concentration (0-100 ppm) on the weight loss of mild steel in hydrochloric acid at different temperatures (35-55°), finding that the corrosion rate decreases with increasing the inhibitor concentration but it increases with increasing the temperature. On the other hand, Al-Fakih [24] evaluated the effect *Curcuma longa L.* concentration (0-10000 ppm) on the weight loss of mild steel in hydrochloric acid at different temperatures (35-65°), finding similar results.

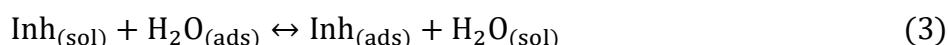
**Table 1.** Electrochemical parameters obtained from the polarization curves in presence of *Curcuma longa L.*

C <sub>inh</sub> (ppm)	E <sub>corr</sub> (mV)	I <sub>corr</sub> (μA/cm <sup>2</sup> )	β <sub>a</sub> (mV/dec)	-β <sub>c</sub> mV/dec	I.E. (%)	θ
0	-464	150	31	75	--	--
100	-510	80	45	159	47	0.47
200	-453	40	49	190	70	0.70
400	-445	20	35	200	86	0.86
600	-445	10	43	206	93	0.93
800	-462	5	24	207	97	0.97
1000	-491	1	34	267	99	0.99

**Table 2.** Electrochemical parameters obtained from the polarization curves in presence of Curcumin.

inh (ppm)	E <sub>corr</sub> (mV)	I <sub>corr</sub> (μA/cm <sup>2</sup> )	β <sub>a</sub> (mV/dec)	-β <sub>c</sub> mV/dec	I.E. (%)	θ
0	-464	150	31	75	--	--
100	-400	40	70	240	65	0.65
200	-430	32	60	300	70	0.70
400	-480	30	55	350	80	0.80
600	-450	20	50	370	85	0.85
800	-440	16	50	350	89	0.89
1000	-440	10	40	300	93	0.93

Since we are assuming that the decrease in the corrosion rate of 1018 carbon steel is due to the adsorption of both *Curcuma longa L.* and Curcumin onto its surface, very important information about the interaction between *Curcuma longa L.* and metal surface can be provided by adsorption isotherms [31]. The adsorption process of the inhibitor is a displacement reaction, where the molecules of the inhibitor replace the water molecules on the metal surface, which can be expressed according to the following equation,



where  $Inh_{(sol)}$  and  $Inh_{(ads)}$  are the inhibitor added in the aqueous solution and adsorbed on the metal surface, respectively.

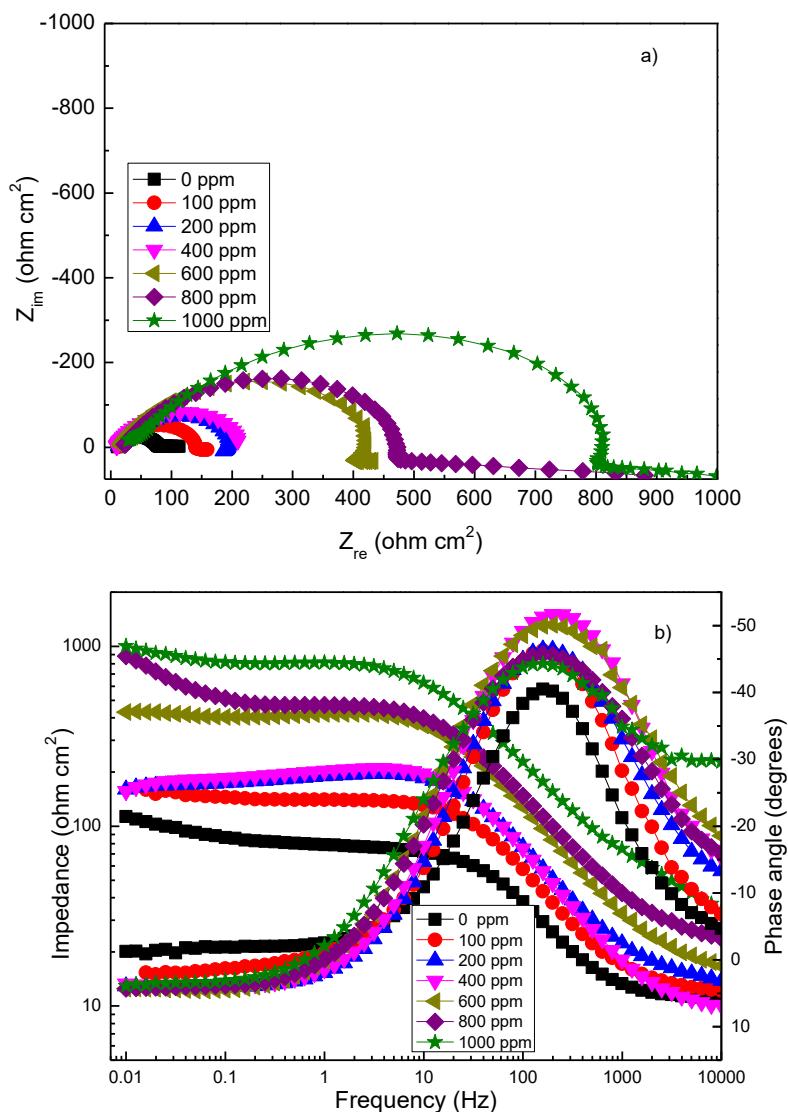


**Figure 8.** Effect of *Curcuma longa L.* concentration on the a) Nyquist and b) Bode diagrams for 1018 carbon steel in 0.5 M H<sub>2</sub>SO<sub>4</sub>.

As observed in data presented in Figure 5, the best fitting was obtained with the Langmuir type of adsorption isotherm. By using Eq. 4 which describes the relationship between the surface coverage,  $\theta$ , which is obtained by dividing the inhibitor efficiency by 100, and the concentration of the inhibitor ( $C_{inh}$ ), the adsorption process at room temperature was found to follow the Langmuir adsorption isotherm:

$$\frac{C_{inh}}{\theta} = \frac{1}{K_{ads}} + C_{inh} \tag{4}$$



$K_{\text{ads}}$  in Eq. 4 is the equilibrium constant of the adsorption process, which can be calculated from the intercept of the fitted line in Fig. 5  $K_{\text{ads}}$  is related to the standard free energy of adsorption ( $\Delta G_{\text{ads}}^0$ ) according to the following equation:

$$\Delta G_{\text{ads}}^0 = -RT \ln (10^6 K_{\text{ads}}) \quad (5)$$

where R is the universal gas constant, T is the absolute temperature, and 10<sup>6</sup> is the concentration of water in the solution in mg/L. The calculated values for  $\Delta G_{\text{ads}}^0$  at room temperature are -16.84 and -19.8 kJ mol<sup>-1</sup> for Curcumin and *Curcuma longa L.* respectively. It has been generally accepted that for values of  $\Delta G_{\text{ads}}^0$  which lie between -20 and -40 kJ mol<sup>-1</sup> the process involved is a weak, physical type of adsorption. On the other hand, for values of  $\Delta G_{\text{ads}}^0$  more negative than -40 kJ mol<sup>-1</sup> involve a strong type of adsorption, i.e., chemisorption [31]. Therefore, a physical type of adsorption, seems to be responsible for the adsorption process of Curcumin and *Curcuma longa L.* on carbon steel.

**Table 3.** Electrochemical parameters used to fit the EIS data obtained in presence of *Curcuma longa L.*

$C_{\text{inh}}$ (ppm)	$R_s$ (ohm cm <sup>2</sup> )	$R_{\text{ct}}$ (ohm cm <sup>2</sup> )	$C_{\text{dl}}$ (F cm <sup>-2</sup> )	I.E. %
0	9	80	3.9E-05	
100	11	146	3.4E-05	45
200	13	190	3.2E-05	57
400	14	196	3.2E-05	59
600	15	400	1.6E-05	80
800	21	510	1.5E-05	84
1000	28	845	1.2E-05	90

### 3.3 Electrochemical measurements

Polarization curves for 1018 carbon steel in 0.5 M H<sub>2</sub>SO<sub>4</sub> containing different *Curcuma longa L.* and Curcumin concentrations are given in Figs. 6 and 7 respectively whereas their electrochemical parameters are given in tables 1 and 2. It can be seen that in both cases anodic branch of the curves display an active behavior without evidence of the formation of a passive layer. The addition of the inhibitor had a marginal effect on the anodic current density value, however, the cathodic current density decreased for almost two orders of magnitude when the *Curcuma longa L.* was added whereas it decreased only one order of magnitude with the addition of Curcumin. The  $E_{\text{corr}}$  value had a marginal effect with the addition of *both inhibitors*. also, since it fluctuated between -445 to -510 mV with the addition of *Curcuma longa L.* and between -445 to -480 mV for the addition of Curcumin, as shown in tables 1 and 2. Inhibitor efficiency, I.E., was calculated by using:

$$\text{I. E. (\%)} = \frac{I_{\text{corr}} - I_{\text{corr}}^{\text{inh}}}{I_{\text{corr}}} \times 100 \quad (6)$$

where  $I_{\text{corr}}$  and  $I_{\text{corr}}^{\text{inh}}$  are the corrosion current density values obtained in absence and presence of the inhibitor. Inhibitor efficiency values increased with an increase in the inhibitor concentration, obtaining a value of 99% with the addition of 1000 ppm of *Curcuma longa L.* and 90% when Curcumin

was added, similar to the results obtained with the weight loss tests. The surface area of metal covered by the inhibitor increases with increasing its concentration also, which indicates that the corrosion inhibition is due to its adsorption on the metal surface.

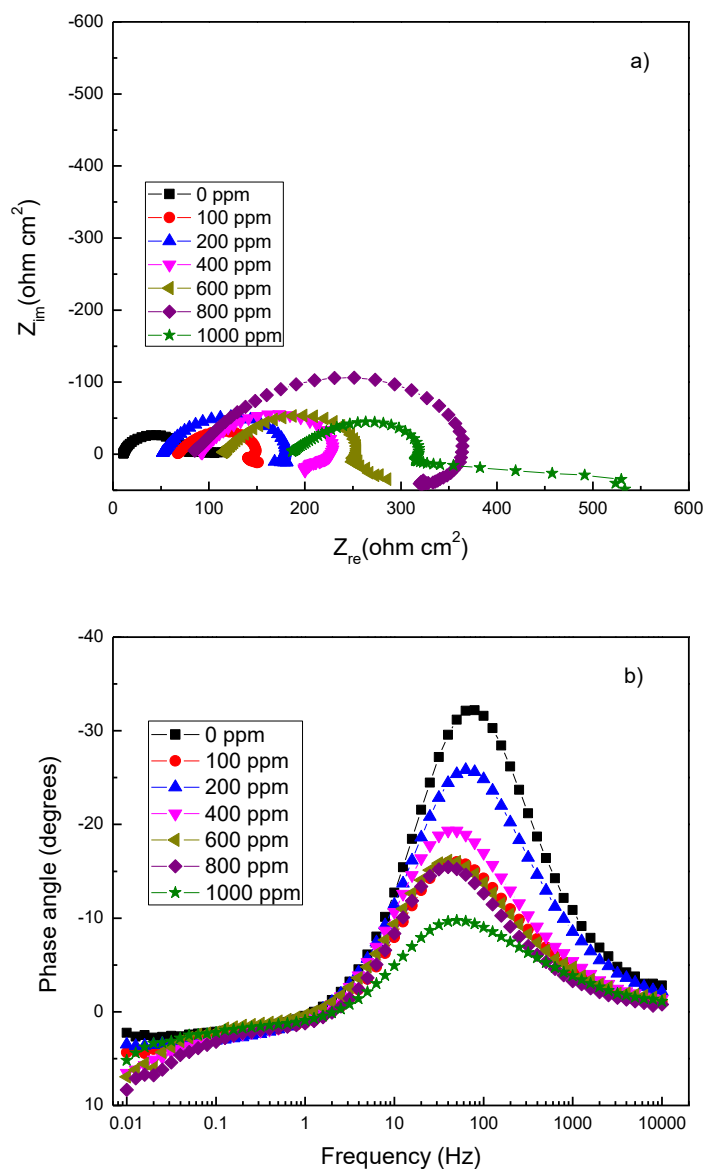


**Figure 9.** Effect of Curcumin concentration on the a) Nyquist and b) Bode diagrams for 1018 carbon steel in 0.5 M H<sub>2</sub>SO<sub>4</sub>.

Anodic Tafel slopes were marginally affected by the addition of *both inhibitors*, however the cathodic ones were dramatically affected. It has been established [26, 27] that if the change in  $E_{corr}$  value induced by the inhibitor addition is more than 85 mV, such a compound could be identified as an anodic or a cathodic type inhibitor. On the contrary, if the shift in the  $E_{corr}$  value is less than 85 mV, then the compound can be considered as mixed type of inhibitor. In our case, the largest shift in the  $E_{corr}$  value is

50 mV when *Curcuma Longa L.* was added, whereas when Curcumin was added, the maximum shift in the  $E_{\text{corr}}$  value was 65 mV, which indicates that the tested extracts performed as mixed-type inhibitors with a predominant cathodic effect as data in tables 1 and 2 indicate. This indicates that both *Curcuma longa L.* and Curcumin diminish the steel anodic dissolution and also retards the hydrogen evolution reaction through blocking the active reaction sites on the steel surface.

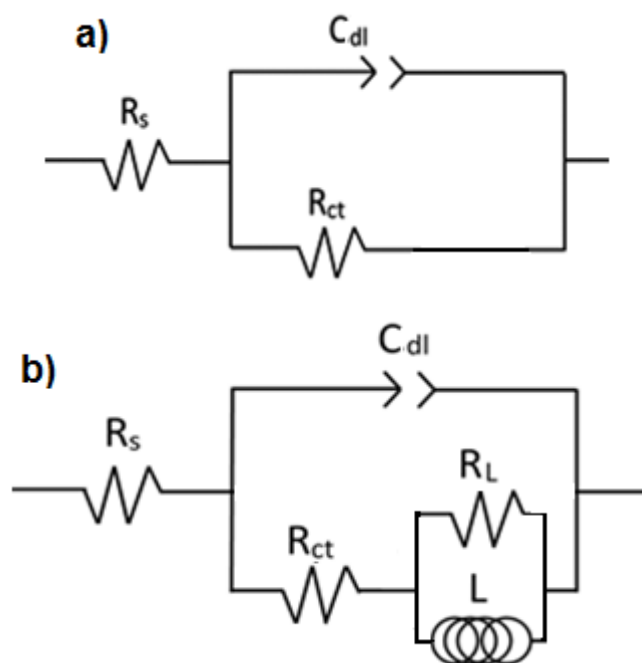


**Figure 10.** Electric circuits used to fit the EIS data for 1018 carbon steel corroded in presence of a) *Curcuma longa L.* and b) Curcumin.

**Table 4.** Electrochemical parameters used to fit the EIS data obtained in presence of Curcumin.

$C_{\text{inh}}$ (ppm)	$R_s$ (ohm $\text{cm}^2$ )	$R_{\text{ct}}$ (ohm $\text{cm}^2$ )	$C_{\text{dl}}$ (F $\text{cm}^{-2}$ )	I.E. %	$R_L$ (ohm $\text{cm}^2$ )	L (H $\text{cm}^{-2}$ )
0	9	80	3.9E-05	--	--	--
100	11	140	3.7E-05	43	13	7
200	13	180	3.2E-05	53	52	29
400	14	230	2.8E-05	65	74	41
600	15	280	1.6E-05	70	79	48
800	21	375	1.4E-05	75	90	59
1000	28	540	1.2E-05	85	107	70

Several researchers have reported different results. Thus, Al-Fakih [24] found that *Curcuma longa L.* decreased the  $I_{\text{corr}}$  value for mild steel in hydrochloric acid from 1587  $\mu\text{A}/\text{cm}^2$  down to 113  $\mu\text{A}/\text{cm}^2$  (an efficiency value of 93%) with the addition of 10,000 ppm of inhibitor but it affected

both the anodic and cathodic Tafel slopes, behaving, thus, as a mixed type of corrosion inhibitor. On the other hand, results obtained by Shahba [28] for mild steel in hydrochloric acid showing a decrease in the  $I_{\text{corr}}$  value from 120 down to 44  $\mu\text{A}/\text{cm}^2$  with the application of 300 ppm of *Curcuma longa L.*, obtaining, thus, an inhibitor efficiency value of 63%. However, the inhibitor behaved as a mixed type of inhibitor affecting mainly the anodic Tafel slope. In our case, the maximum efficiency value, 99%, was obtained with the addition of 1000 ppm of *Curcuma longa L.*, but it behaved as a cathodic-dominant mixed type of inhibitor. On the other hand Al-Amiery [29] evaluated the addition of a curcumin derivative, i.e. (1E,4Z,6E)-5-chloro-1,7-bis(4-hydroxy-3-methoxyphenyl)hepta-1,4,6-trien-3-one (chlorocurcumin), as corrosion inhibitor for mild steel in hydrochloric acid, obtaining efficiency values as high as 78%, behaving as a mixed type of inhibitor. Inhibitor efficiency increased with increasing the inhibitor concentration but it decreased with rising the testing temperature. In addition to this, in another work [30] used different curcumin derivatives, i.e. 1,7-Bis-(4-hydroxy-3-methoxy-phenyl)-hepta-1,6-diene-4-arylo-3,5-dione in the corrosion inhibition of brass in nitric acid. They found that the inhibitors efficiency increased with their concentration and they were adsorbed on to the metal Surface according to a Frumkin type of adsorption isotherm. Inhibitors behaved as mixed type but affecting mainly the cathodic electrochemical reactions.

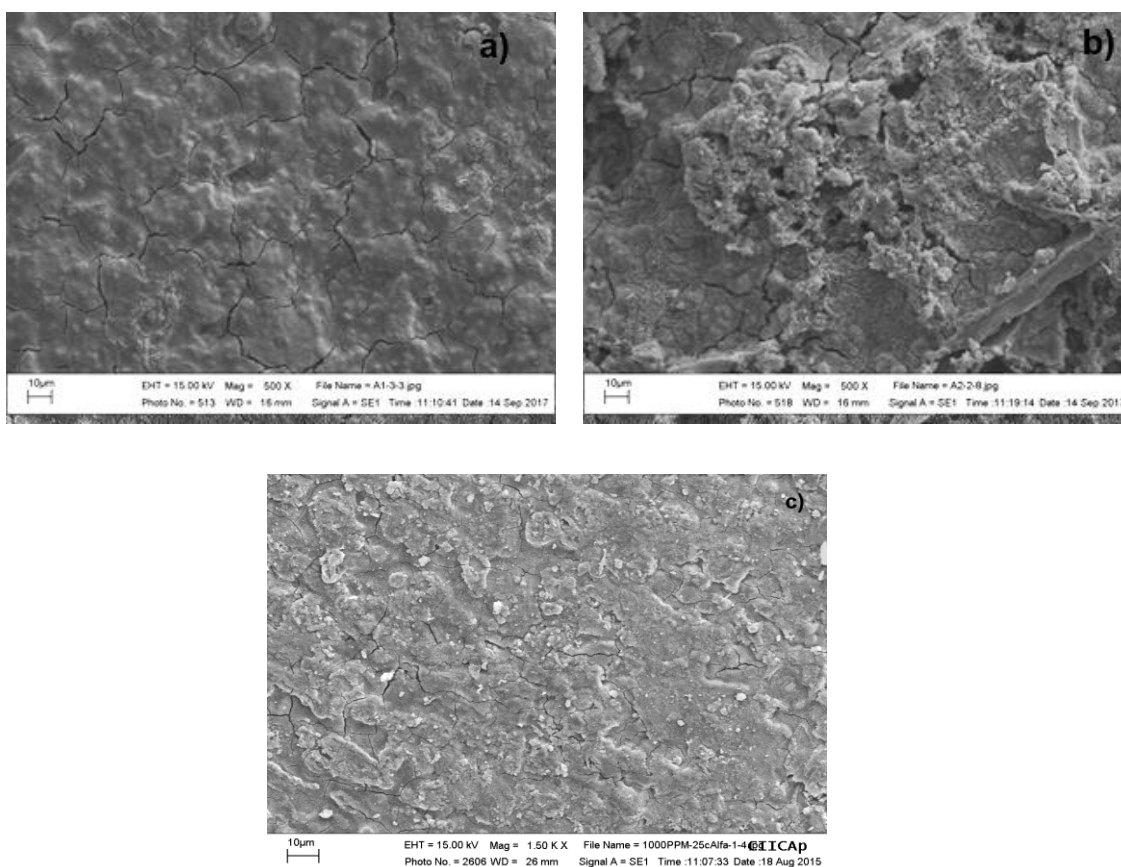


**Figure 11.** SEM micrographs of 1018 carbon steel samples corroded in 0.5 M H<sub>2</sub>SO<sub>4</sub> solution in presence of a) 0 ppm, b) 1000 ppm of *Curcuma longa L.* and c) 1000 ppm of Curcumin.

EIS data in both Nyquist and Bode formats for 1018 carbon steel in 0.5 M H<sub>2</sub>SO<sub>4</sub> containing different concentrations of *Curcuma longa L.* and Curcumin are given in Figs. 8 and 9. Nyquist diagrams for the tests with *Curcuma longa L.* extract, Fig. 8 a, display a single capacitive loop at all frequency values with their centers at the real axis, indicating a charge transfer controlling process which is not affected by the presence of the inhibitor. On the other hand, Nyquist diagrams in presence of Curcumin, Fig. 9 a, display a capacitive semicircle at high and intermediate frequency values followed by an inductive loop at lower frequency values, indicating that the corrosion process is under controlled by the adsorption/desorption of some intermediate species work [31, 32]. The diameter loop increases as the inhibitor concentration increases, which is due to the adsorption of the inhibitor and the formation of a protective film, reaching its maximum value with 1000 ppm of inhibitor. In some inhibitor concentrations, it can be seen that the real impedance increases whereas the imaginary part remains constant, which is due to the accumulation of corrosion products at the steel [31, 32]. The semicircles are not perfect which is due to dispersion effects due to roughness and inhomogeneous of the surface electrode. In addition to this, it can be seen that the real axis intercept at high frequencies in the presence of inhibitor is bigger than that in the absence of inhibitor (blank solution) and increases as the inhibitor concentration increases. This indicates that the impedance of inhibited substrate increases with increasing the inhibitor concentration. On the other hand, Bode diagrams, Fig. 8 b and 9 b, show only one peak around 100 or 200 Hz, and thus, only one time constant. This peak increases in its phase angle value and the frequency interval is broader as the inhibitor concentration increases. EIS data can be modeled by using electric circuits shown in Fig. 10. In these figures, R<sub>s</sub> is the solution resistance, R<sub>ct</sub> the charge transfer resistance and C<sub>dl</sub> the double layer capacitance, L the inductance and R<sub>L</sub> its resistance. Electrochemical parameters used to fit EIS data by using circuits shown in Fig. 10 are given in tables 3 and 4. It can be seen that R<sub>ct</sub> increases, which is due to more impediment of the active area at the metal surface as a result of the increase in inhibitor concentration [29, 30], whereas the C<sub>dl</sub> value decreases with the inhibitor concentration. This result is somehow expected since R<sub>ct</sub> and C<sub>dl</sub> are inversely proportional according to:

$$C_{dl} = (2\pi f_{max} R_{ct})^{-1} \quad (7)$$

where  $f_{max}$  is the frequency value where the maximum value of imaginary impedance is found. On the other hand, an alternative way to calculate C<sub>dl</sub> is by using following equation:

$$C_{dl} = \epsilon \epsilon_0 A / \delta \quad (8)$$

where  $\epsilon$  is the double layer dielectric constant,  $\epsilon_0$  the vacuum electrical permittivity,  $\delta$  the double layer thickness, and A the surface area. A decrease in the C<sub>dl</sub> value can be due to a decrease in the double layer dielectric constant, a decrease in the surface area or to an increase in the double layer thickness. Due to the fact that the process is not under diffusion control, the later is not possible, and the surface area is, in this case, constant, therefore the decrease in the C<sub>dl</sub> value is attributed to the replacement of the adsorbed water molecules at the surface metal by the inhibitor having lower dielectric constant [33] which indicates that the adsorption of the inhibitor molecules is necessary to decrease the steel corrosion rate.

### 3.4 Surface characterization

Micrographs of corroded 1018 carbon steel specimens in absence and presence of 1000 ppm of *Curcuma longa L.* and Curcumin are shown in Fig. 11, whereas micro chemical analysis of the corrosion products film are given in Fig. 12.

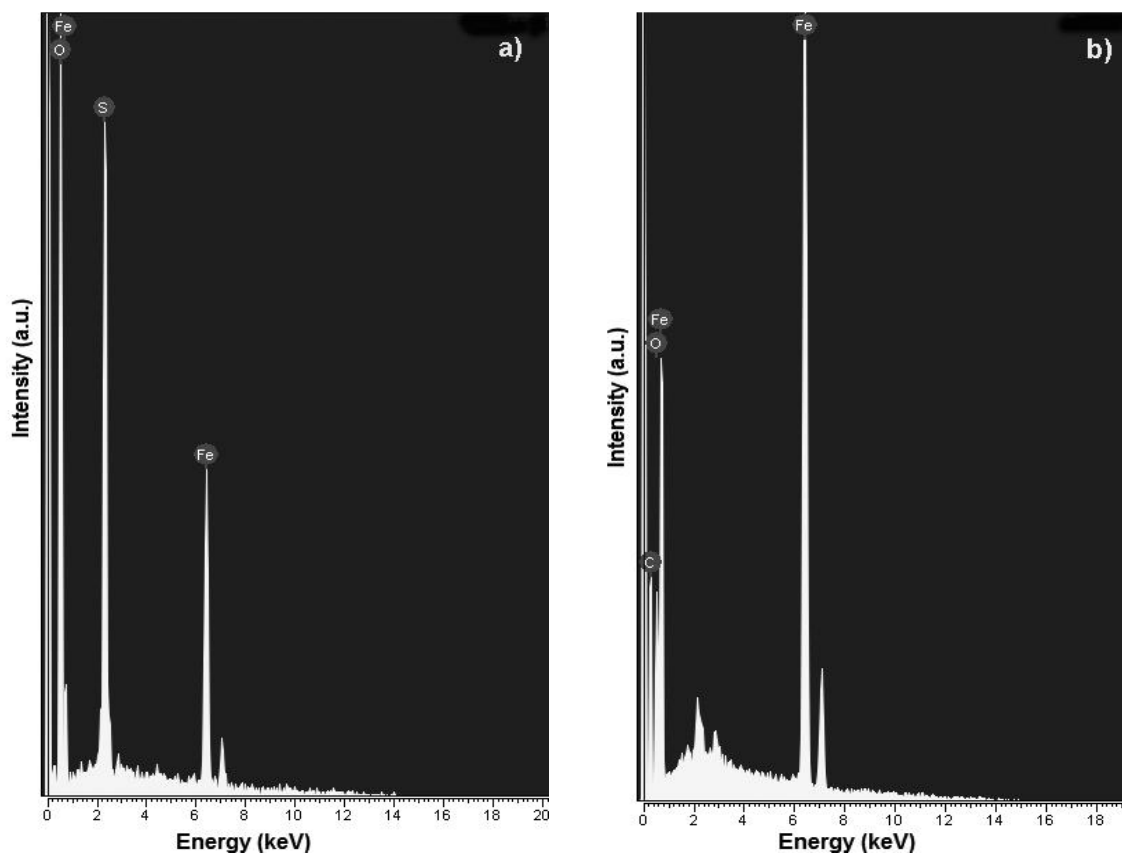


**Figure 12.** EDX chemical analysis of the corrosion products for specimens corroded in a) absence and b) presence of 1000 ppm of *Curcuma longa L.*

For specimen corroded in the uninhibited solution, Fig. 11 a, corrosion products film present a big amount of micro cracks and pores which form paths for the aggressive solution to penetrate it and corrode the underlying metal. On the other hand, corrosion products film formed on top of specimen corroded in presence of 1000 ppm of *Curcuma longa L.* and Curcumin, Fig. 11 b and c, are more compact, with a much less amount of micro cracks and micro pores, protecting, thus, the underlying metal from the aggressive action of electrolyte. Micro chemical analysis carried out on the corrosion products formed on top of specimen corroded in the uninhibited solution, Fig. 12 a, indicates the presence of Fe, O, and S, elements present either on the steel or in the electrolyte. For specimen corroded in presence of *Curcuma longa L.* extract, Fig. 12 b, chemical analysis shows that in addition to the elements from the environment or in the steel, there is the presence of C, which is only present in an organic compound, in this case, the *Curcuma longa L.* extract. This confirms the fact that the reduction

in the corrosion rate of 1018 carbon steel in 0.5 M H<sub>2</sub>SO<sub>4</sub> solution is due to the adsorption of a protective film containing *Curcuma longa L.* on top of the steel.

#### 4. CONCLUSIONS

The present study has revealed that extract of *Curcuma longa L.* as well as Curcumin are good corrosion inhibitors for 1018 carbon steel in 0.5 M H<sub>2</sub>SO<sub>4</sub> solution since they efficiently decreased the steel corrosion rate by forming a protective film which is physically adsorbed on top of the steel surface following a Langmuir type of adsorption isotherm. Both inhibitors affected both anodic and cathodic reactions, but they had a stronger effect on the later, behaving thus, as a mixed type of inhibitors with a dominant cathodic effect. Inhibitor efficiency increased with an increase in its concentration, reaching higher values with *Curcuma longa L.* than those for Curcumin. The inhibition efficiency of both inhibitors is due to the presence of heteroatoms present in these compounds.

#### References

1. J.A. Calderon, F.A. Vasquez, J.A. Carreño, *Mater. Chem. Phys.*, 185(2017) 218.
2. F. El-Hajjaji, M.E. Belghiti, B. Hammouti, S. Jodeh, O. Hamed, H. Lgaz, R. Salghi, *Portugaliae Electrochimica Acta*, 36(2018)197.
3. M. Mahdavian, S. Ashhari, *Electrochim. Acta*, 55(2010)1720.
4. Sumayah Bashir, Vivek Sharma, Hassane Lgaz, Ill-Min Chung, Ambrish Singh, Ashish Kumar, *J. Mol. Liq.* 263 (2018) 454.
5. A. Kahyarian, A. Schumaker, B. Brown, S. Nesic, *Electrochim. Acta* 258 (2017) 639.
6. Chandrabhan Verma, Lukman O. Olasunkanmi, Eno E. Ebenso, M.A. Quraishi, *Results in Physics*, 8 (2018) 657.
7. Eiman Alibakhshi, Mohammad Ramezanzadeh, Ghasem Bahlakeh, Bahram Ramezanzadeh, Mohammad Mahdavian, Milad Motamedi, *J. Mol. Liq.*, 255 (2018) 185.
8. Simona Varvara, Roxana Bostan, Otilia Bobis, Luiza Gaina, Florin Popa, Vicente Mena, Ricardo M. Souto, *Appl. Surf. Sci.*, 426 (2017) 1100.
9. Patricia E. Alvarez, M. Victoria Fiori-Bimbi, Adriana Neske, Silvia A. Brandán, Claudio A. Gervasi, *J. Ind. Eng. Chem.*, 58 (2018) 92.
10. A. Saxena, D. Prasad, R. Haldhar, G. Singh, A. Kumar, *J. Env. Chem. Eng.*, 6 (2018) 694.
11. G. Khan, K.Md. S. Newaz, W. J. Basirun, H. B. M. Ali, F. L. Faraj, G. M. Khan, *Int. J. Electrochem. Sci.*, 10 (2015) 6120.
12. R. Haldhar, D. Prasad, A. Saxena, *J. Env. Chem. Eng.*, 6 (2018) 2290.
13. G.N. Roth, A. Chandra, M.G. Nair, *J. Nat. Prod.*, 61 (1998) 542.
14. A.C.C.M. Manzan, F.S. Toniolo, E. Bredow, N.P. Povh, *J. Agric. Food Chem.*, 51 (2003) 6802.
15. G. Began, M. Goto, A. Kodama, T. Hirose, *Food Res. Int.*, 33(2000) 341.
16. R. Priya, A. Prathapan, K.G. Raghu, A.N. Menon, *Asian Pac. J. Trop. Biomed.*, 2 (2012) S695.
17. A. Gupta, S. Mahajan, R. Sharma, *Biotechnol. Rep.*, 6 (2015) 51.
18. T.T. Dao, P.H. Nguyen, H.K. Won, E.H. Kim, J. Park, B.Y. Won, *Food Chem.*, 134 (2012) 21.
19. M.I. Balbi-Peña, A. Becker, J.R. Stangarlin, G. Franzener, M.C. Lopes, K.R.F. Schwan-Estrada, *Fitopatol. Bras.*, 31 (2006) 3.
20. S. Khattak, H. Saeed-ur-Rehman, W. Ullah Shah, M. Ahmad, *Fitoterapia*, 76 (2005) 254.
21. S.Y. Park, D.S.H.L. Kim, *J. Nat. Prod.*, 65 (2002) 1227–1231.
22. M.E.M. Braga, P.F. Leal, J.E. Carvalho, M.A.A. Meireles, *J. Agric. Food Chem.*, 51 (2003) 6604.

23. Nurul Izni Kairi, Jain Kassim, *Int. J. Electrochem. Sci.*, 8 (2013) 7138.
24. A.M. Al-Fakih, M. Aziz, H.M. Sirat, *J. Mater. Environ. Sci.*, 6 (2015) 1480.
25. C. Verna, L. O. Olasunkanmi, E. E. Ebenso, M. A. Quraishi, *Results in Physics* 8 (2018) 657.
26. Z. Tao, S. Zhang, W. Li, B. Hou, *Corros. Sci.*, 51 (2009) 2588.
27. S.A. Pauline, S. Sahila, C. Gopalakrishnan, S. Nanjundan, N. Rajendran, *Prog. Org. Coat.*, 72 (2011) 443.
28. Rabab Mohamed Abou Shahba, Abd El-Aziz El-Sayed Fouda, Azza El-Sayed El-Shenawy, Amina Salah Mohamed Osman, *Mat. Sci. App.*, 7(2016) 654.
29. A.A: Al-Amiery, A.A.H. Kadhum, A.B. Mohamad, A.Y. Musa, Ch. J. Li , (2013), *Materials*, 2013(2013) 5466.
30. A.S. Fouda, K.M. Elattar, (2012), *J. Mat. Eng. Perf.*, 21(2012) 2354.
31. M. Özcan, I. Dehri, M. Erbil, *Appl. Surf. Sci.*, 236 (2004) 155.
32. R. Solmaz, G. Kardas, M. Culha, B. Yazıcı, M. Erbil, *Electrochim. Acta*, 53(2008) 5941.
33. E. Poorqasemi, O. Abootalebi, M. Peikari, F. Haqdar, *Corros. Sci.*, 51(2009) 1043.

© 2019 The Authors. Published by ESG ([www.electrochemsci.org](http://www.electrochemsci.org)). This article is an open access article distributed under the terms and conditions of the Creative Commons Attribution license (<http://creativecommons.org/licenses/by/4.0/>).